Materials Research Proceedings 54 (2025) 946-955 https://doi.org/10.21741/9781644903599-101

Study of correlation between scraps and main process parameters in flow-forming alloy wheels production

Alessandro Trevisani[1,a], Andrea Abeni[1,b*], Paola Serena Ginestra[1,c], Alessio Franchi[2,d], Alessandro Concoreggi[2,e], Mauro Silvestri[2,f], Elisabetta Ceretti[1,g]

[1]Department of Mechanical and Industrial Engineering, University of Brescia, Via Branze 38, 25123 Brescia, Italy

[2]Cromodora Wheels S.p.a., via Montichiari 20, 25016 Ghedi (BS), Italy

[a]a.trevisani001@studenti.unibs.it, [b]andrea.abeni@unibs.it, [c]paola.ginestra@unibs.it, [d]afranchi@cromodorawheels.com, [e]aconcoreggi@cromodorawheels.com, [f]msilvestri@cromodorawheels.com, [g]elisabetta.ceretti@unibs.it

Keywords: Flow-Forming, Automotive, Alloy Wheels, Light Alloys, DOE, Quality Management

Abstract. Flow-forming is a metalworking process that can be employed to produce lightweight, high-strength components by plastically deforming materials using circumferential and axial forces. This technique is employed in the automotive industry, particularly for wheel manufacturing, allowing a reduction of weight and an enhancement of the mechanical properties. The process has been extensively studied to investigate its influence on the final properties such as tensile strength, surface roughness, and fatigue resistance. However, challenges such as residual stress, defects, and micro-cracks remain crucial for optimizing final product quality. The study investigates the defects distribution after flow-forming of aluminium alloy (AlSi7Mg0.3) wheels. The process involves heating pre-formed wheels to a target temperature higher than 400°C, followed by controlled plastic deformation using two rollers that reshape the material. Data on the process, such as spindle speed, material temperature, and machine downtimes, were collected from five flow-forming stations over a 23-week production period. Analysis of the data was conducted using the statistical methods ANOVA and DOE to correlate process variations with the occurrence of defects on products. Once the most impactful process parameters were identified, FEM methods were utilized to correlate the parameters with the temperature distribution in the parts and with the geometry achieved by the deformation. Furthermore, the numerical model of the process was utilized to investigate the effects of machine downtimes, defining a methodology to individuate and tackle the most relevant issues in flow-forming processes.

Introduction

The application of flow-forming process to manufacture aluminium wheels is crucial to enhance the vehicle efficiency and its overall performance, since they are characterized by higher mechanical properties and a substantial weight reduction compared to traditional cast wheels [1]. Several studies [2,3] estimate a reduction of weight equal to 10-15% due to introduction of flow-forming on cast blanks instead of using only the casting process. While initially the lightweight attracted motorsport applications [4], the advantages of an improved acceleration response and an enhanced power-to-weight ratios are now extended to a wider range of automotive applications. Furthermore, the reduction of unsprang mass implicates a lower fuel consumption of vehicles. As demonstrated by recent investigations [5], lightweight wheels contribute significantly to the energy efficiency of vehicles and enhance their sustainability. In addition to weight reduction, flow-forming technology improves mechanical strength and fatigue resistance. Flow-formed aluminium

alloys exhibit up to a 60% increase in tensile strength and up to a 50% increase in hardness, if compared with conventional cast material [6]. This improvement results from the controlled plastic deformation induced by the compressive loads, which refines the microstructure of the material and reduces the internal defects, such as porosity and inclusions. A study [7] on the fatigue behaviour of flow-formed A356-T6 alloy highlighted as these microstructural enhancements lead to greater impact resistance and durability of components, further mitigating crack propagation. Another important advantage related to the application of flow-forming on wheels is the superior surface finish compared to other forming and machining techniques [8]. The process reduces the roughness of the cast blanks due to the pressure of the rollers, which plastically deform the material and smooth the surface irregularities. Additionally, the rotary action of the material during deformation acts as a dynamic polishing mechanism.

To achieve all these advantages, it is crucial to strictly optimize and control the process, its parameters and its tools, in order to maximize the quality and the properties, and to avoid the occurrence of defects. The maintenance of the pre-heating temperature above 400°C ensures optimal material deformability, without determining excessive friction with rollers. The temperature control is crucial also to achieve target mechanical properties and preventing premature tool wear [9]. In [10] was verified as excessive feed rates can lead to surface undulations and deviations in circularity tolerance. Moreover, roller dimensions impact the quality of the process, as larger rollers allow to cover greater surface areas for each tool pass and to increase the grain structure homogenization, but it results also in difficulties about control the pressure distribution and the temperature [11]. Additionally, excessive roller attack angle induces aggressive deformation, which can increase surface friction and temperature, potentially compromising surface quality [12]. During the process, the tools undergo to high pressure and repeated contact which determines roller wear. It is the results of the combination of abrasion, adhesion, fatigue, and oxidation. Strategies to mitigate roller wear involve selecting high-hardness materials, applying surface coatings, optimizing lubrication, and fine-tuning process parameters such as rotational speed and attack angle, but production downtimes are necessary to substitute the worn tools.

Despite its advantages, the flow-forming process is not without challenges. Material backflow, inadequate material flow, and ovality, defined as the deviations from the perfect circularity, can result from an incorrect alignment of rollers or as a consequence of excessive deformation rates [13]. Furthermore, wrinkling is a recurrent defect in flow-forming which arises as surface folds due to localized instability. Gupta et al. [14] identify inadequate mandrel support and excessive roller feed rates as primary causes. Optimizing feed rates, introducing intermediate annealing, and ensuring sufficient mandrel support can mitigate wrinkling by improving the stability of the deformation. Flow-forming can also induce residual stress distribution along the inner and outer surfaces of the wheel which have a negative effect on the fatigue resistance. In [15], Jiang et al. experimentally and numerically verify as in a flow-formed wheel the transverse stresses remain minimal, while circumferential stresses can range between 100 and 150 MPa, concentrated near tensioned zones. Nevertheless, the number of studies related to defectiveness related to flow-forming process are limited and they regard only a small number of tests conditions and repetitions.

These defects underscore the importance of precise control over process parameters. Advanced numerical models, such as finite element methods (FEM), can be applied to simulate the flow-forming process, allowing precise predictions of temperature distributions, material behaviour, and resulting geometries [16,17]. The FE modelling of flow-forming is a challenging procedure due to the typical limits related to the numerical modelling of complex processes, such as the high computational time. For this reasons, only a few researches related the numerical modelling of flow-forming can be find in literature. In this study, an extensive ANOVA analysis was conducted on process data to identify the factors correlated with defect occurrence with a robust statistic

method. By analysing parameters such as spindle speed, cooling bath temperature, and internal flange temperature, the study highlighted their relative impact on specific defect types, enabling targeted optimization of the flow-forming process. To deep investigate the influence of key parameters, process variations and downtimes, the cooling process before flow-forming was modelled with a FEM software. Furthermore, also the flow-forming process was modelled to numerically investigate the correlation between process conditions, geometry profiles, and defect occurrence. This approach enabled a detailed evaluation of critical scenarios, highlighting strategies to mitigate defects and optimize the flow-forming process. The procedure highlighted which process parameters in flow-forming are more related to the occurrence of defects and, at the same time, offers a robust methodology to tackle the non-conformities and to improve the yield of the process.

Material and Methods

The production system analysed in this study consists of five identical stations for flow forming. The machine employed, visible in Fig. 1 (a), is a two-roller model from LEIFELD (WSC 650/4H), able of producing wheels with a diameter ranging from 16 to 24 inches. The machine has a rotating spindle, which supports the raw wheel blank, as visible in the details shown in Fig. 1 (b). This spindle is composed of a flange, head, guide sleeve, and actuator, along with a tailstock that secures the blank. The tailstock assembly comprises a flange, a pressure foot, and an internal pressure plate. A roughing roller and a finishing roller are positioned opposite each other, at a 180° angle relative to the feed axis. The rotating tools have identical geometric shapes, with a diameter of 360 mm and a width of approximately 60 mm.

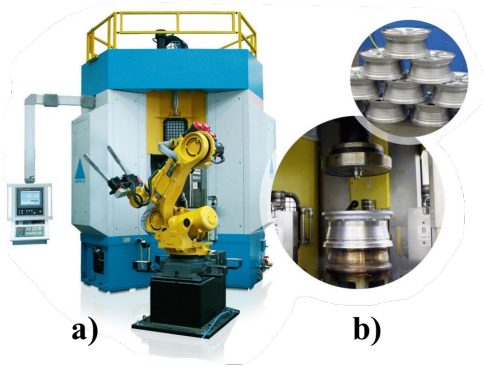

Figure 1 – The flow-forming station (a) and a detail of the rotating spindle supporting a wheel (b).

Each station is equipped with two robots: one for loading and one for unloading the wheels. The wheel blank is initially heated in a furnace to a target temperature T_t for a pre-heating period. This phase increases the ductility of the material by thermal softening before the flow-forming process. Higher ductility reduces the force required during roller pass and it allows a stricter control of the plastic deformation of the wheel. Subsequently, the robot transfers the heated wheel to a water-cooling tank with a controlled temperature T_{tk}, where only the rim of the wheel is not immersed. After cooling, the same robot loads the wheel into the flow-forming machine, where annular rolling of the wheel rim occurs through plastic deformation. Upon completion of the flow-forming process, the second robot removes the wheel from the machine and immerses it in a controlled temperature water bath for complete cooling. Finally, the robot places the cooled wheel on a roller conveyor for transportation out of the flow-forming area. The processed material is the aluminium alloy AlSi7Mg0.3 (ENAC-42100) with an average tensile strength of 230-290 MPa and the chemical composition listed in Table 1.

Table 1 – Chemical composition of AlSi7Mg0.3.

Fe	Si	Mn	Ti	Cu	Mg	Zn	Al
Max 0.19	*6.5-7.5*	*Max 0.1*	*Max 0.25*	*Max 0.05*	*0.25-0.45*	*Max 0.07*	*Remainder*

To deep investigate the defect and non-conformity, a dataset related to a production of over 23 weeks was considered. The non-conformities are detected with go-no go inspections and they are classified in three groups: start-up defects are geometrical or dimensional non-conformities which usually occurs at the restart of the flow-forming process; the witness marks, which are located on the wheel rim, are detected after the machining and are determined by an inadequate machining allowance; the deformation defects are related to the wheel spokes and are determined by a deformation of the outer rim during the flow-forming. The dataset collects process information related to each wheel, and it was aggregated to compute, for each production lot, the maximum, the minimum, the average and the standard deviation of each recorded parameter. The study was performed by assuming that only the following data could influence the defect:

- Internal flange temperature after cooling, before flow-forming T_{if}.
- Cooling bath temperature T_{tk}.
- Cooling tank liquid flow rate FR_{tk}.
- Spindle rotational speed ω.
- Spindle power consumption P_{spin}.

The material of the wheels was not considered as only one aluminium alloy is employed. The complete dataset was then correlated with the non-conformity data due to the defects identified in different production lots. The defect dataset is organized as follows:

- Lot data: code, production start date, and end date.
- The machine employed for the lot
- Number of non-conformities due to start-up defects, witness marks, and deformations.
- Total number of non-conformities related to flow-forming.

Minitab© software was used to analyse the relationship between process parameters and production non-conformities through ANOVA analysis. Initially, a box plot was created using the data from the five flow-forming stations to examine the distribution of the defects and to assess the homogeneity of the data population. Subsequently, the process data were classified into intervals to allow the identification of correlations or trends.

Particular attention was attributed to the internal flange temperature T_{if}, which was hypothesized as a primary cause of defects. To investigate start-up defects an interaction plot was used, by considering as independent factors the machine employed and T_{if}. Further analyses focused on witness mark non-conformities through main effects plots, examining the minimum, maximum and average values of T_{if} for each production lot. The same methodology was applied to evaluate non-conformities caused by deformations.

The defects distribution was also investigated in relation to the wheel diameter, aiming to determine which size exhibited the highest scrap percentage, for each typology of defect and absolutely both. This was followed by an investigation of correlations between wheel size and the average value of T_{if}. Similar analyses were performed also for the rim height.

The effect of spindle rotational speed on non-conformities was also assessed. On one hand, excessively high speeds could overheat the wheel, raising temperatures and potentially concurring to determines defects. On the other hand, low spindle speeds could result in insufficient force to deform the wheel, leading to process inefficiencies and poor product quality. Finally, ANOVA was employed to evaluate the impact of machine stoppages on total non-conformities and on witness mark scrap for each lot. Only the stoppage of a period equal to 10 times and 20 times the cycle period were considered.

Materials Research Proceedings 54 (2025) 946-955 https://doi.org/10.21741/9781644903599-101

To understand the relationships between process variables and defects, two FEM models were developed by using ProCAST 3D© software to model the temperature distribution in the wheel resulting from the cooling after the furnace heating, and FORGE© software to simulate the flow-forming process.

The thermal simulations of cooling were used to investigate the effect on the thermal distribution of three factors, the furnace exit temperature, the cooling bath temperature and the cooling tank liquid flow rate. Standard values, respectively T_t, T_{tk}, FR_{tk}, were defined for each of the three factors and subsequently the simulations were performed by varying only one parameter at a time, on four levels for the furnace exit temperature and on three for the other factors, keeping other parameters at standard conditions. The ranges of each parameter were selected by considering the actual variations in the real process, since there is a strict control of the furnace exit temperature, the cooling bath temperature and the cooling tank liquid flow rate. Table 2 summarizes the combination of the factors which were simulated. The air heat transfer coefficient was set equal to 15 W/m^{2}K. The 2.5D axial symmetric thermomechanical simulations of flow-forming were used to understand how the temperature distributions influence the resulting geometry, especially the rim thickness. The workpiece was modelled as plastic material with 2500 tetrahedral elements, while the mandrel, the tailstock and the rollers are modelled as rigid bodies. A heat transfer coefficient of the air was set equal to 10 W/m^{2}K. The contact with the mandrel and tailstock was modelled with a Columb friction (μ=0.4) and a heat transfer coefficient of 5000 W/m^{2}K, while the contact with the rollers was modelled with a Tresca friction (m=0.9) and a heat transfer coefficient of 1000 W/m^{2}K. They represent the standard setting suggested by the FE software for a plastic deformation process.

Table 2 – Condition of process parameter employed in FE simulations.

Test	Furnace exit temperature (°C)	Cooling bath temperature (°C)	Cooling tank liquid flow rate (l/min)
Standard	T_t	T_{tk}	FR_{tk}
Decreased T_t	T_t *-10°C*	T_{tk}	FR_{tk}
Increased T_t	T_t *+10°C*	T_{tk}	FR_{tk}
Max T_t	T_t *+35°C*	T_{tk}	FR_{tk}
Decreased T_{tk}	T_t	T_{tk} *-15°C*	FR_{tk}
Increased T_{tk}	T_t	T_{tk} *+15°C*	FR_{tk}
Increased FR_{tk}	T_t	T_{tk}	FR_{tk}*+5 l/min*
Max FR_{tk}	T_t	T_{tk}	FR_{tk}*+15 l/min*

Results and Discussion

The annual average total scrap rate across the entire production is designated as Annual Non-Conformities *AnC%*. To ensure a more homogeneous dataset, the lots with a non-conformity higher than three times *AnC%* (3**AnC%*) were considered outliers and excluded from the analysis. Among the five flow-forming stations, FF5 exhibited the highest scrap rate, averaging 1.2**AnC%*, followed by FF1 at 1.05**AnC%*, while the remaining three stations recorded scrap rates below 0.8**AnC%*% as visible in Fig. 2 (a). These values confirm the homogeneity of the dataset due to their limited variability among the flow-forming stations. The analysis of interaction between start-up defects and the temperature of the internal flange temperature T_{if} (Fig. 2 (b)) revealed consistent trends across the stations, with one exception: station FF4 and especially FF5 displayed a significant increase in start-up non-conformities when temperatures exceeded T_t + 20°C, which can be derived by an overheating in the furnace combined with an uncorrected cooling process. Fig. 3 summarizes the relation between witness marks (a) and deformation defects (b) and T_{if}. The witness marks peaks as the average internal flange temperature T_{if} ranges between T_t - 10°C and T_t + 10°C, suggesting as the cooling should slightly reduce the temperature also in this area.

Interestingly, temperatures higher than T_t + 10°C minimizes witness, but they are not desirable because as previously discussed overheating increases start-up non-conformities. Finally, non-conformities caused by deformation appeared less sensitive to variations in T_{if}.

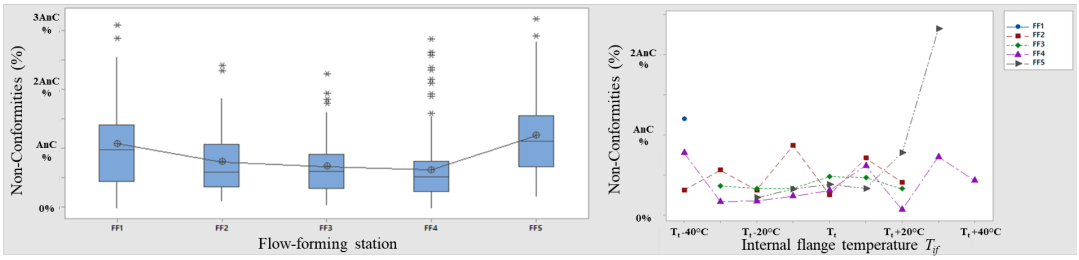

(a) (b)

Figure 2 – Box plot of total defects on each f-f station (a) and the interaction plot of non-conformities with T_{if} (b).

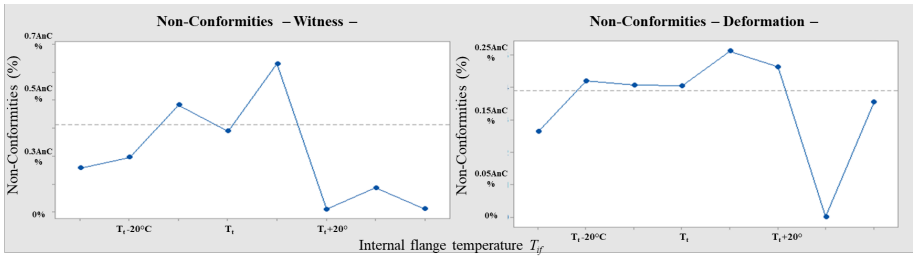

(a) (b)

Figure 3 – The main effect plot of T_{if} on witness marks (a) and on deformation defects (b).

About the effect of the wheel dimension, Fig. 4 shows as start-up non-conformity (a) were most prevalent for the diameter of 19 inches, witness mark scraps (b) peaked for the diameter 21 inches, and deformation defects (c) were most significant for diameter 20 inches. Notably, diameter 21 consistently displayed elevated scrap rates across all categories, and consequently it was chosen for the numerical investigation.

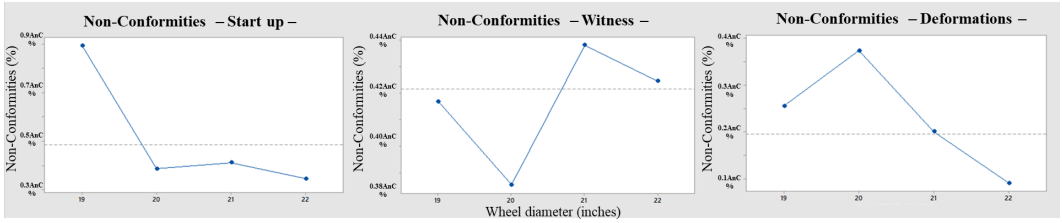

(a) (b) (c)

Figure 4 – The main effect plot of the wheel diameter on start-up non-conformities (a), witness marks (b), deformation defects (c).

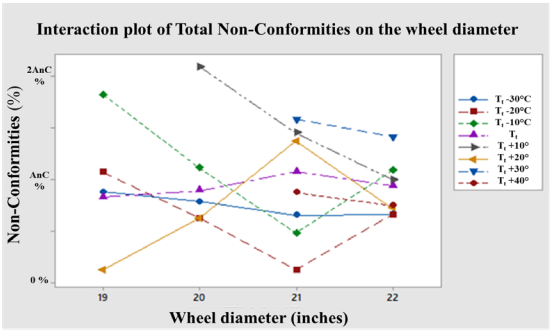

Figure 5 – The interaction plot of the wheel diameter on total non-conformities at different T_{if}.

Fig. 5 shows as the values of temperature T_{if} higher than T_t + 10°C are correlated with the highest total non-conformities for diameters 20, 21, and 22 inches. However, the distribution of temperature ranges was irregular, and no specific trends emerged. About the rim height, Fig. 6 (a) indicated a significant increase in total non-conformities, deformation scraps, and witness mark for rim higher than 11 inches, which consistently exceeded the average. This rim height is utilized exclusively in 21 inch diameter wheels, corroborating earlier findings that these wheels produced the highest overall scrap rates. Consequently, a relationship between rim height, wheel diameter, and scrap rates was confirmed. Fig. 6 (b) shows as, for the 11-inch rim wheels, the maximum amount of non-conformities occurred at temperatures higher then T_t. This trend was consistent across specific defects categories. These findings suggest that highest wheel dimensions (21-inch diameter and 11-inch rim height) maximizing process defects as their temperature T_{if} are less reduced by cooling, if compared with smaller wheels with a lower thermal inertia.

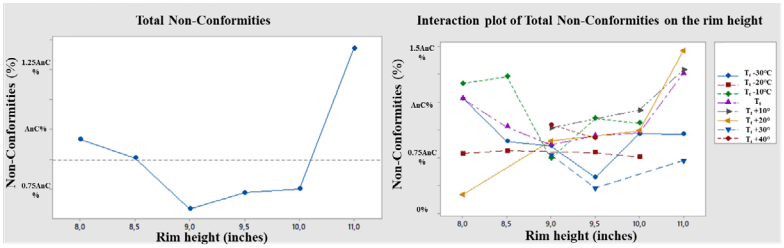

(a) (b)

Figure 6 – The main effect plot of the rim height on total scrap (a) and the interaction plot of the rim height on total non-conformities at different T_{if}.

Spindle rotational speed analysis is visible in Fig. 7. Two peaks were identified, corresponding to ω_1 (absolute peak) and ω_2=1.10 ω_1. The stratification of the data by non-conformity type highlights as at ω_1 the peak for witness mark is recorded, while the start-up defect maximum occurs at ω_2.

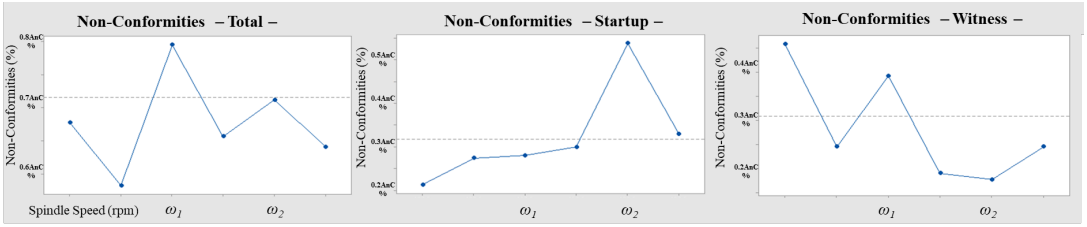

(a) (b) (c)

Figure 7 – The main effect plot of the spindle speed on the total scrap (a), and the main effect plot of the spindle speed limited to the start-up defect (b) and witness mark (c).

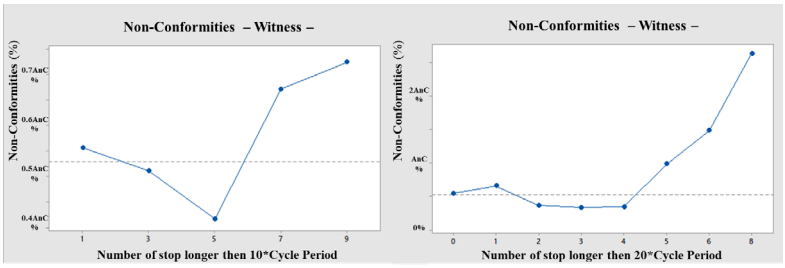

(a) (b)

Figure 8 – The main effect plot of the machine downtimes higher than 10 times the cycle period (a) and 20 times the cycle period (b) on the witness mark non-conformities.

ANOVA analysis of machine downtimes revealed that total scraps remained near the average for minimal stoppages. However, a proportional increase in total scraps was observed with downtimes exceeding 10 times and especially 20 times the cycle period. Fig. 8 shows the trend in particular for witness mark defects, which increased with extended downtimes more than the other factors. The FEM analysis allowed to verify as also the downtimes impacts of the defects occurrence. From the analysis of the production data clearly emerged a correlation between non-conformities and the temperature of the wheel after cooling which was further investigated by the FEM modeling of the cooling. It was applied to a wheel geometry corresponding to D = 21 inches and h = 11 inches, since they were the dimensions associated with the highest defects occurrence. The aim of the simulations was to understand if the possible variations of the process parameters might have influenced the internal flange temperature, since it resulted correlated to the occurrence of non-conformities. Fig. 9 (a) shows how the temperature distribution along the profile of the wheel changes by considering different temperature at the furnace exit. Under standard condition of furnace temperature T_t, the area of the rim with a temperature varying between 95% and 100% of T_t covered approximately one-third of its height (see Fig. 9 (a)). At maximum temperature T_t + 35°C, the hottest region expanded to over half the rim height. The high temperature of the rim predominantly influenced start-up and witness mark defects, which are located in this part of the wheels. Consequently, stricter control of the furnace temperature appears profitable.

Fig. 9 (b) summarizes the effects of the temperature of the cooling bath on the temperature distribution along the profile of the wheel. The variation of T_{tk} determines a modification of the temperature distribution limited to the external rim edge. Furthermore, the maximum variation of temperature is equal to 10°C, consequently it is possible to state that the cooling bath temperature has a minimal thermal impact on the non-conformities.

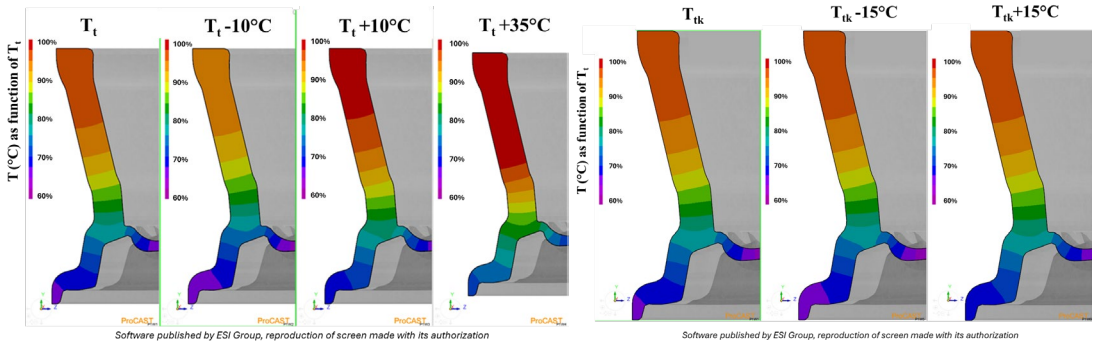

(a) (b)

Figure 9 – FEM simulation of temperature distribution along the profile of the wheel at different temperature at the furnace exit (a) and at different temperature of the cooling bath (b).

About the fluid flow rate, an increase of FR_{tk} increases the cooling speed, expanding the cooled area on the rim. On one hand the temperature in the central zone changes up to 75 °C, but on the other hand the temperature distribution in the internal flange remained unchanged, as visible in Fig. 10 (a). It is possible to conclude that flow rate variations do not have an impact on start-up or witness mark scraps. To further investigate the effect of production halts on scrap rates, simulations were conducted using Forge by considering a downtime equal to 20 times the cycle period. During this interval, the mandrel was assumed to cool uniformly, resulting in an average temperature drop of approximately 70°C, as visible in Fig. 10 (b) and (c). The flow-forming process was simulated by combining the temperature profile of the wheel achieved at T_t + 35°C (Fig. 9(a)) with the temperature profile of the mandrel after the downtime (Fig. 10 (c)), and a comparison of the wheel profile with the standard scenario was performed.

In standard scenarios, the thermal expansion of the spindle reduces the gap between the wheel blank and mandrel, enabling accurate flow forming and achieving the desired rim thicknesses. After a restart of the machine, the reduced spindle temperature following extended downtimes led to spindle contraction, increasing the gap and resulting in incomplete flow forming. Rim thickness increases of 0.4 mm causing incomplete deformation in the upper wheel sections. This confirmed that downtimes exceeding 20 times the cycle period without spindle reheating significantly elevated witness mark scraps.

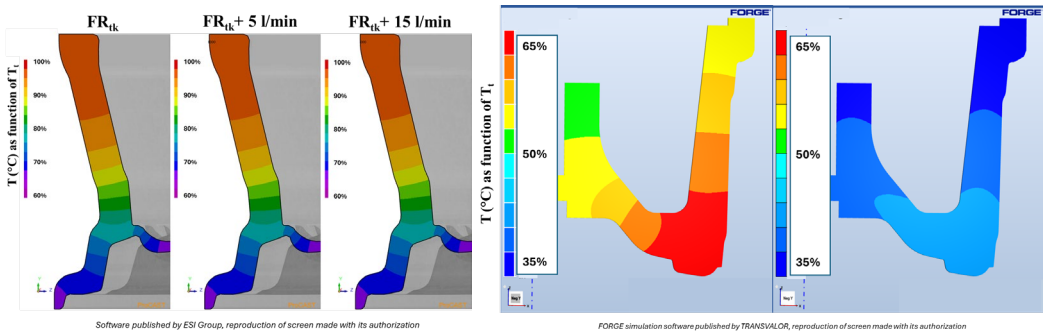

(a) (b) (c)

Figure 10 – FEM simulation of temperature distribution along the profile of the wheel at different cooling tank liquid flow rates (a); temperature distribution along the profile of the mandrel in regime conditions (a) and after a downtime of 20 times the cycle period (b).

Conclusions

Flow forming represents a critical advancement in metalworking technology, offering unmatched benefits in weight reduction, mechanical performance, and surface finishing. The study successfully established significant correlations between the occurrence of production defects in flow-formed alloy wheels and key process parameters. By combining statistical methods such as ANOVA with numerical simulations, the analysis revealed that the internal flange temperature after cooling is related with the non-conformities. This finding highlights the necessity for stringent temperature control throughout the process, starting from furnace exit to post-cooling stages. Extended machine downtimes resulted as another impact factor, leading to spindle contraction and incomplete flow-forming. The integration of thermal and mechanical simulations provided a comprehensive understanding of these interactions, offering practical insights for optimizing process conditions. In conclusion, this study underlines the critical role of process parameters in enhancing the quality and efficiency of flow-forming operations, giving an input for more robust manufacturing strategies and reduced scrap rates in alloy wheel production.

Acknowledgement

Financed by the European Union - NextGenerationEU (National Sustainable Mobility Center CN00000023, Italian Ministry of University and Research Decree n. 1033 - 17/06/2022, Spoke 11 - Innovative Materials & Lightweighting). The opinions expressed are those of the authors only and should not be considered as representative of the European Union or the European Commission's official position. Neither the European Union nor the European Commission can be held responsible for them. CUP D83C22000690001.

References

[1] M. Kleiner, M. Geiger, A. Klaus, Manufacturing of lightweight components by metal forming, CIRP Ann. Manuf. Technol. 52 (2003) 521-542. https://doi.org/10.1016/S0007-8506(07)60202-9

[2] S.Y. Hwang, N. Kim, C.S. Lee, Numerical investigation on the effect of process parameters during aluminum wheel flow-forming, Stroj. Vestn. - J. Mech. Eng. 61 (2015) 471-476. https://doi.org/10.5545/sv-jme.2014.2180
[3] W.J. Chen, Y. Xu, H.W. Song, S.H. Zhang, S.F. Chen, L.L. Xia, et al., A novel hydroforming process by combining internal and external pressures for high-strength steel wheel rims, Materials 15 (2022) 6820. https://doi.org/10.3390/ma15196820
[4] M. Zanchini, D. Longhi, S. Mantovani, F. Puglisi, M. Giacalone, Fatigue and failure analysis of aluminium and composite automotive wheel rims: Experimental and numerical investigation, Eng. Fail. Anal. 146 (2023) 107064. https://doi.org/10.1016/j.engfailanal.2023.107064
[5] K. DeMarco, J. Stratton, K. Chinavare, G. VanHouten, The Effects of Mass and Wheel Aerodynamics on Vehicle Fuel Economy, SAE Tech. Pap. (2017) 2017-01-1533. https://doi.org/10.4271/2017-01-1533
[6] H.R. Molladavoudi, F. Djavanroodi, Experimental study of thickness reduction effects on mechanical properties and spinning accuracy of aluminum 7075-O, during flow forming, Int. J. Adv. Manuf. Technol. 52 (2011) 949-957. https://doi.org/10.1007/s00170-010-2782-4
[7] M.J. Roy, D.M. Maijer, J. Zhao, Fatigue characterization of flow-formed A356-T6, MATEC Web Conf. 12 (2014) 03001. https://doi.org/10.1051/matecconf/20141203001
[8] D. Marini, D. Cunningham, J. Corney, A review of flow forming processes and mechanisms, Key Eng. Mater. 651 (2015) 750-758. https://doi.org/10.4028/www.scientific.net/KEM.651-653.750 https://doi.org/10.4028/www.scientific.net/KEM.651-653.750
[9] A. D'Annibale, A. Di Ilio, A. Paoletti, D. Paoletti, S. Sfarra, The combination of advanced tools for parameters investigation and tools maintenance in flow forming process, Procedia CIRP 59 (2017) 144-149. https://doi.org/10.1016/j.procir.2016.09.038
[10] M.J. Davidson, K. Balasubramanian, G.R.N. Tagore, Experimental investigation on flow-forming of AA6061 alloy-a Taguchi approach, J. Mater. Process. Technol. 200 (2008) 283-287. https://doi.org/10.1016/j.jmatprotec.2007.09.026
[11] M. Haghshenas, M. Jhaver, R.J. Klassen, J.T. Wood, Plastic strain distribution during splined-mandrel flow forming, Mater. Des. 32 (2011) 3629-3636. https://doi.org/10.1016/j.matdes.2011.02.014
[12] M. Jahazi, G. Ebrahimi, The influence of flow-forming parameters and microstructure on the quality of a D6ac steel, J. Mater. Process. Technol. 103 (2000) 362-366. https://doi.org/10.1016/S0924-0136(00)00508-2
[13] M. Srinivasulu, M. Komaraiah, C.S.K.P. Rao, Experimental studies on the characteristics of AA6082 flow-formed tubes, J. Mech. Eng. Res. 4 (2012) 192-198.
[14] R.K. Gupta, B.R. Ghosh, V.A. Kumar, M.K. Karthikeyan, P.P. Sinha, Investigation of cracks generated during flow forming of Nb-Hf-Ti alloy sheet, J. Fail. Anal. Prev. 7 (2007) 424-428. https://doi.org/10.1007/s11668-007-9089-2
[15] Q. Jiang, Z. Zhao, Z. Xu, J. Sun, X. Chen, B. Su, et al., Effect of residual stresses on wheel fatigue life and experimental validation, Machines 10 (2022) 924. https://doi.org/10.3390/machines10100924
[16] M. H., Parsa, A. A. Pazooki, M. Nili Ahmadabadi, Flow-forming and flow formability simulation, The International Journal of Advanced Manufacturing Technology 42 (2009) 463-473. https://doi.org/10.1007/s00170-008-1624-0
[17] C. Cappellini, L. Giorleo, G. Allegri, A. Attanasio, E. Ceretti, A digital twin approach to automotive wheel flow forming process, In International Symposium on Industrial Engineering and Automation (2022) 114-126. Cham: Springer International Publishing. https://doi.org/10.1007/978-3-031-14317-5_10